

Numerical investigation of clean and ice-accreted aerofoils at low Reynolds number and low angle of attack

N.L.Oo, P.J.Richards, R.N.Sharma

Department of Mechanical Engineering

University of Auckland, Auckland 1142, New Zealand

Abstract

In order to investigate the aerodynamic behaviour arising from the icing of UAV wings, a numerical simulation was conducted on a RG15 aerofoil using Large Eddy Simulation (LES) at a Reynolds number of 1×10^5 . The investigation was conducted on both a clean and an ice-accreted aerofoil, at 0° and 6° angles of attack (AoA). It is found that even at very low angles of attack, the leading-edge ice accretion causes the formation of an ice induced separation bubble (ISB) which generates leading-edge vortices at a very high frequency. The formation of laminar separation bubble (LSB) was not observed at 0° AoA for the clean aerofoil, where the flow was separated through the trailing-edge. As the iced aerofoil angle of attack was increased to 6° , the size of the ISB lengthened, reattaching to the surface further downstream. In contrast, the laminar separation from the clean aerofoil moved towards the leading-edge. The formation of the ISB at the leading-edge of the iced aerofoil forced the boundary layer to immediately become turbulent at both 0° and 6° AoA, in contrast to the laminar boundary layer formed ahead of the LSB for the clean aerofoil. As expected, the boundary layer on the clean aerofoil was turbulent after the reattachment of the LSB.

Introduction

Aerial vehicles are generally designed to operate in many types of meteorological conditions. Operating under extreme weather conditions is an unavoidable factor for many aircraft. Icing is the most common problem associated with flying vehicles when the surrounding temperature is lower than water freezing point (0°C). In recent years research on Unmanned Aerial Vehicles (UAVs) has surged because of its applicability in a broad spectrum of applications ranging from household to military operations. However, the huge potential of UAVs gets constrained when they have to operate under adverse weather conditions, for example, when the vehicle is under severe turbulence and/or icing condition [1]. To avoid this scenario in unmanned aircraft and micro aerial vehicles (MAVs), it has been suggested not to fly under icing weather conditions as no promising technique has been developed to overcome performance deterioration. According to Szilder and Mcilwain [2], UAVs are normally designed to cruise at low altitude as well as low flying velocity which increases the duration for ice formation on the surface.

With accretion of ice on the lifting surfaces of an aircraft, the aerodynamic profile of the wing gets altered, which results in unsteadiness in the flow field, decreases the

maximum lift coefficient and increases the drag coefficient, along with premature stall. The significant aerodynamic challenges induced by the presence of the leading-edge ice accretion in the stagnation region has attracted the interest of several researchers [3-8]. This includes a variety of ice shapes accreted at the leading edge, and a range of Reynolds number from 0.5×10^6 to 1.8×10^6 . Liu and Wang [8] show that the maximum lift reduces drastically (by up to 63.9%) due to the presence of leading-edge ice while Jackson and Bragg [9] report that the drag coefficient increases up to 486% compared to the clean aerofoil. Maximum lift is further reduced by premature stall. Sometimes in extreme icing condition, stall can occur even at very low AoA, as low as 3° [8].

Flying fixed wing aircraft at low Reynolds numbers comes with several challenges. The obvious example is the flow transition from laminar to turbulence while in flight. Depending on the shape and position (inclination angles) of an aerofoil, the formation of laminar separation and reattachment is often observed. The form of Laminar Separation Bubbles (LSB) depends strongly on the aerofoil geometry and its flying speed at a range of Reynolds number starting from 5×10^4 to 3×10^6 [10]. The adverse pressure gradient resulting laminar separation induces an increment of drag and flow instabilities. The form of separation bubble is typically classified into short and long bubbles [11]. Short LSBs are found at higher angles of attack whereas long bubbles occur at lower angles of attack. On the other hand, having ice accretion at the leading-edge of an aerofoil forces a separation bubble known as Ice-induced separation bubble (ISB). Brag et al [12] suggest the characteristics of the ISB are similar to that of laminar separation bubble (LSB) which is formed due to the adverse pressure gradient. Unlike an LSB, which moves upstream with an increase of the angle of attack, the size of an ISB tends to increase with increasing AoA. Consequently, the separated flow from the ISB promotes leading-edge vortices even at lower angles of attack [13]. This further induces a drag increment and flow instabilities around the profile.

This study aims to address the instabilities of the ice induced separations at low Reynolds number in comparisons with the well-known instabilities of the laminar separation bubble.

Numerical Simulations

Numerical simulations were carried out on a clean and an ice-accreted RG-15 aerofoil. The ice accretion model at the leading-edge of the RG-15 aerofoil was adopted from

one of the previous studies conducted by Williams et al. [3] at low Reynolds number. The ice was generated according to the standard of Federal Aviation Regulation (FAR) Appendix C to Part 25 [14] in an icing tunnel. The reference altitude was kept at 5000 ft at an air velocity of 14.3 m/s with zero inclination angle, and the generated 0° CM (continuous maximum) ice shape is shown in Figure 2.



Figure 1 Leading edge 0-deg Continuous Maximum ice accretion on RG-15 aerofoil adopted from Williams et al. [3]

The chord of the reference aerofoil (without ice accretion) was $c=210\text{mm}$ which corresponds to a Reynolds number of 1.07×10^5 at an air velocity of 7.25 m/s with inviscid irrotational boundary condition at the inlet. A sub-grid scale model is used in the current study using LES (wall-adapting local eddy viscosity)[15]. For the numerical solver option, a central difference method was employed in ANSYS CFX [16].

The size of the domain was kept the same for both ice accretion and clean aerofoil cases. In both cases, a C-grid domain was employed with a $3c$ radius for the inlet and the outlet/opening located $6c$ downstream from the reference leading-edge of the aerofoil. The size of the domain was sufficiently large to be numerically independent, but as small as possible to reduce the computational cost. As the LES was solved in 3-D, the domain's span should be wide enough for a 3-dimensional flow to be developed fully. According to Frere et al. [17], the domain for LES is sufficient if the span is equivalent to 10.5% of the chord. In this study, an aerofoil span of 11.4% of the reference chord was used which also gives room for the chord length extension due to the ice accretion. The numerical domain is shown in Figure 3.

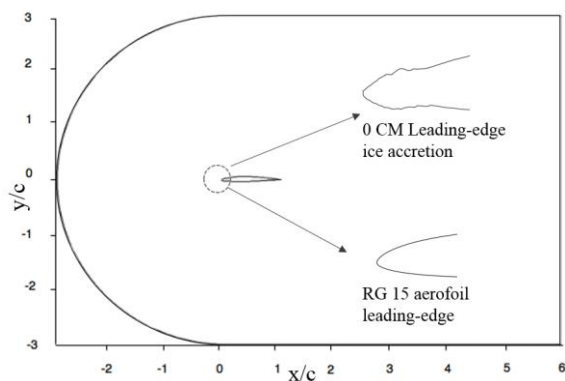


Figure 2 Schematic diagram of numerical domain

The computational domain was meshed using ICEM CFD according to the requirement of the LES for transitional flow where the chord-wise resolution was kept at $16 \leq \Delta x^+ \leq 27$, with higher concentration near the leading and trailing edges. The spanwise direction was meshed uniformly with $\Delta z^+ \sim 12$ and the $\Delta y^+ < 1$. This leads to a

total of 12 million elements for the clean aerofoil case and approximately 12.5 million elements for the ice accretion case.

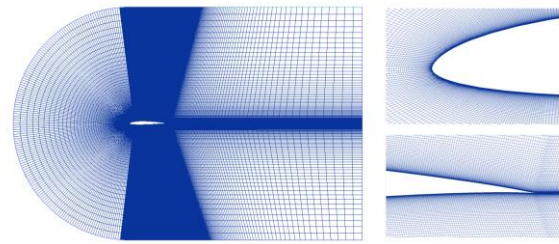


Figure 3 Reference aerofoil, RG-15 mesh

Large eddy simulation of a transitional flow requires a sufficiently small time step to allow the solver to resolve all the small eddies present in the flow field. For the current study, a numerical time step of $5 \times 10^{-5} s$, equivalent to a maximum Courant-Friedrichs-Lewy (CFL) of 0.44 [18] was employed which gives a total of 20,000 samples per second. After performing a Fast Fourier Transformation (FFT), the maximum frequency of 10,000Hz will be acquired which is sufficient to develop the flow field for obtaining the maximum frequency of interest which is less than 1000Hz in this study. The numerical stability was usually obtained at 4000 time steps. For obtaining the high-resolution spectra, the steady numerical simulation data was collect up to 16,000 time steps.

Results and Discussion

The formation of separation can be observed either from the wall shear stress (skin friction coefficient) or the pressure coefficient. In this study, pressure coefficient was used for determining the separation and reattachment locations of the separation bubbles, ISB and LSB respectively. The major differences between the two separation bubbles are – the LSB starts to form well downstream on the aerofoil and gradually moves towards the leading edge with increasing AoA, whereas, the ISB always starts to form immediately downstream of the ice which is near the leading edge for leading-edge ice accretion case. The ISB on the leading edge grows gradually as the angle of attack (AoA) increases. A unique property of LSB is the transformation into a short separation bubble when the bubble approaches the leading-edge at higher AoA, whereas, the size of the ISB increases with the increase in angle of attack (shown in Figure 4 (b and d)).

At 0° AoA, an ISB was observed on the ice-accreted aerofoil due to backward facing step created by leading-edge ice. However, for the clean aerofoil, while no formation of laminar separation bubble was found, the flow is observed to be separated from the trailing-edge (shown in Figure 4(a)).

At 6° AoA, a LSB was formed at the upstream of the clean aerofoil which reattached back to the surface at $0.4c$ as shown in Figure 4(c).

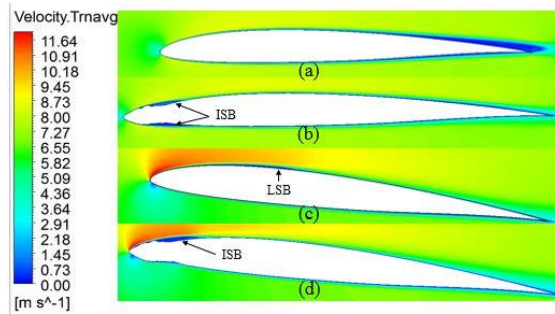


Figure 4 Average velocity contour illustrating the formation of separation bubbles (a) 0° reference (b) 0° ice-accreted (c) 6° reference (d) 6° ice-accreted

The formation of either ISB or LSB on the profile surface instantly changes the laminar boundary layer (before separation) to a turbulent boundary layer (after reattachment). Figure 5 represents the pressure coefficient, C_p , distributions for both configurations i.e. reference an ice-accreted aerofoil at 0° and 6°. Under ice-accretion, the presence of a distinct plateau confirms the presence of flow separation, namely the ISB, at both AoA where the flow was instantly separated from the $0c$ location of the reference aerofoil. That separated flow goes under transitional stage at approximately $0.08c$ for 6° and $0.07c$ for 0° AoA, can be seen from the pressure plateau in Figure 5. This further reattaches to the surface at about $0.09c$ at 0° and $0.12c$ at 6° AoA which signifies the increase in AoA increases the size of the Ice-induced separation.

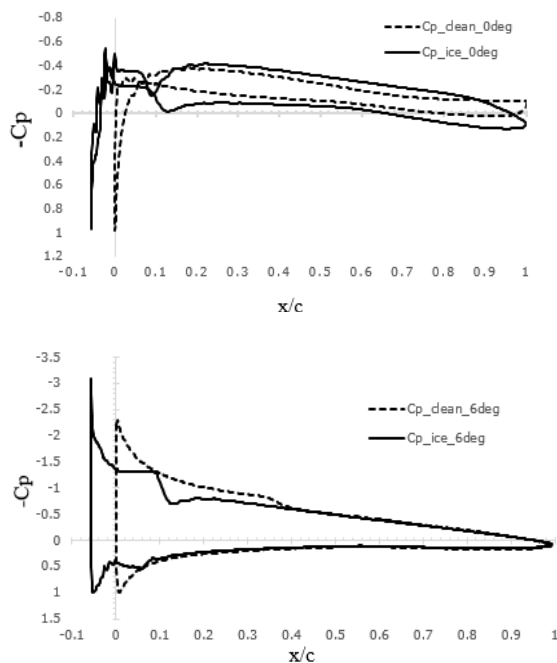


Figure 5 Pressure Coefficient comparisons between the reference clean aerofoil and ice-accreted aerofoil at 0° (top) and 6° (bottom) AoA

Instabilities at ISB and LSB

After the separation of the shear-layer, it goes into a phase of transition which has been found from pressure coefficients in both ISB and LSB. The instabilities in the transitional region have been studied extensively. The transition is a region where the two-dimensional flow breaks down into three-dimensional instabilities. Before reaching the three-dimensional instability, the flow field inside the transitional region possess a high frequency oscillation. These phenomena have been reported by many researchers [11, 19-21].

A similar pattern of instabilities was observed in the ice induced separations as well, in the present study. It is found that the fundamental (instability) frequency increases at the ISB transition from 597 Hz at 0° to 633 Hz at 6° AoA; see the power spectra plotted in Figure 7.

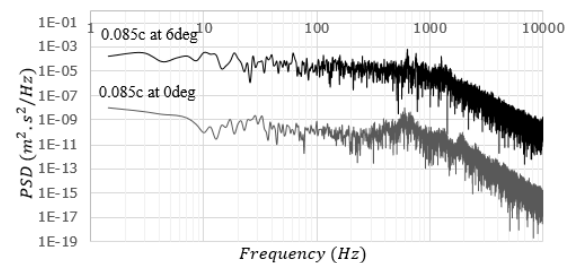


Figure 6 PSD at the transitional location of Ice-induced separation bubble taken at $y/c = 0.001$. 0° is decreased by three order of magnitude for clarity

As mentioned previously, a laminar separation bubble does not form on the clean aerofoil at 0° AoA, however, a transitional type of instability was found at the trailing edge with the fundamental frequency of 537 Hz; see Figure 8. After the trailing edge, the flow quickly transformed into turbulence with 3-dimensional instability. For 6° AoA, the transitional regime is found to be similar to the conventional transition process with the flow oscillation at 651Hz.

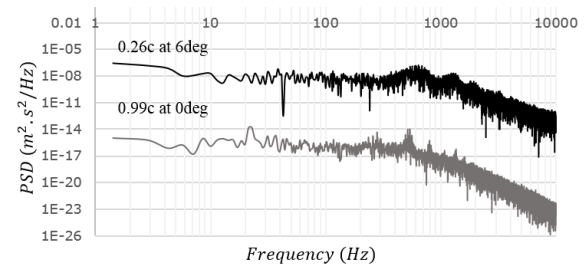


Figure 7 PSD at the transitional location of laminar separation bubble taken at $y/c = 0.001$. 0° is decreased by three order of magnitude for clarity

The Fundamental frequency obtained at the transitional separation has been non-dimensional in terms of Strouhal number, $St = fl/U_0$, where, f is the fundamental frequency, l is the projected high of aerofoil on vertical plane (or aerofoil thickness) and U_0 is the freestream velocity.

According to Gerakopoulos [22] and LeBlanc [19], the Strouhal number increases with the increase in angle of attack for the same Reynolds number. In this study with two different angles of attack, an increment in Strouhal number has been found at the transitional flow regime with the increase in aerofoil angle of attack. The increase in the Strouhal number on the clean aerofoil was found to be higher than that of the ice accreted aerofoil; see Figure 9.

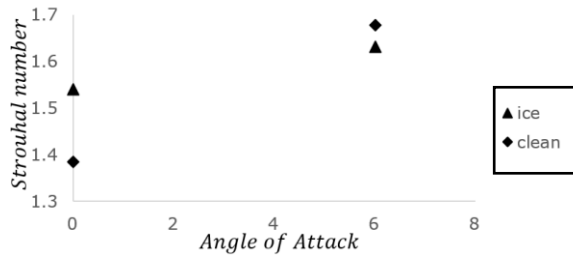


Figure 8 Variation in Strouhal number according to angle of attack at $Re=100,000$

Conclusion

Large Eddy Simulations of a clean (reference) and an ice-accreted aerofoil have been conducted at 0° and 6° AoA to investigate the formation of ice-induced and laminar separation bubbles, ISB and LSB. Both separation bubbles formed at a low Reynolds number possess similar characteristics which are the result of adverse pressure gradient on the profile. Especially at low Reynolds number, it was obvious from the pressure coefficient distribution, that the ISB also exhibits transitional behaviour before reattaching to the surface, and these phenomena are similar to that around the backward facing step. The transitional region in the ISB was found to be dominated by high frequency oscillations, similar to that of LSB where the fundamental frequency increases with the increase in Angle of attack. In the case of the reference clean aerofoil at 0° AoA, while a LSB was not found, a transitional behaviour was nevertheless observed at the trailing-edge. It can also be concluded that, the process of transition is almost identical in both LSB and ISB's.

Acknowledgments

The author would like to thank to Nesi (New Zealand eScience Infrastructure) for providing access to the high computational processors for numerical simulations.

References

- Szilder, K. and W. Yuan. *The Influence of Ice Accretion on the Aerodynamic Performance of a UAS Airfoil*. in *53rd AIAA Aerospace Sciences Meeting*. 2015.
- Szilder, K. and S. McIlwain, *In-Flight Icing of UAVs-The Influence of Reynolds Number on the Ice Accretion Process*. 2011, SAE Technical Paper.
- Williams, N., et al. *The effect of icing on small unmanned aircraft low Reynolds number airfoils*. in *17th Australian International Aerospace Congress: AIAC 2017*. 2017. Engineers Australia, Royal Aeronautical Society.
- Chung, J. and J. Addy, Harold. *A numerical evaluation of icing effects on a natural laminar flow airfoil*. in *38th Aerospace Sciences Meeting and Exhibit*. 2000.
- Kim, H.S. and M.B. Bragg, *Effects of leading-edge ice accretion geometry on airfoil performance*. AIAA paper, 1999: p. 99-3150.
- Ansell, P.J. and M.B. Bragg, *Unsteady Modes in Flowfield About Airfoil with Horn-Ice Shape*. *Journal of Aircraft*, 2015. **53**(2): p. 475-486.
- Gurbacki, H.M. and M.B. Bragg, *Unsteady aerodynamic measurements on an iced airfoil*. AIAA paper, 2002. **241**: p. 2002.
- Liu, C. and Y. Wang, *Numerical analysis of ice accretion effects at super-cooled large droplet conditions on airfoil aerodynamics*. *Journal of Modern Transportation*, 2011. **19**(4): p. 274-278.
- Jackson, D.G. and M.B. Bragg. *Aerodynamic performance of an NLF airfoil with simulated ice*. in *AIAA, Aerospace Sciences Meeting and Exhibit, 37 th, Reno, NV*. 1999.
- Hain, R., C. Kähler, and R. Radespiel, *Dynamics of laminar separation bubbles at low-Reynolds-number airfoils*. *Journal of Fluid Mechanics*, 2009. **630**: p. 129-153.
- Malkiel, E. and R. Mayle. *Transition in a separation bubble*. in *ASME 1995 International Gas Turbine and Aeroengine Congress and Exposition*. 1995. American Society of Mechanical Engineers.
- Bragg, M., A. Khodadoust, and S. Spring, *Measurements in a leading-edge separation bubble due to a simulated airfoil ice accretion*. AIAA journal, 1992. **30**(6): p. 1462-1467.
- Gurbacki, H.M., *Ice-induced unsteady flowfield effects on airfoil performance*. 2003.
- Wright, W.B., *User Manual for the NASA Glenn Ice Accretion Code LEWICE. Version 2.2*. 2. 2002.
- Ducros, F., F. Nicoud, and T. Poinsot, *Wall-adapting local eddy-viscosity models for simulations in complex geometries*. 1998, Oxford University Computing Laboratory, Oxford, UK. p. 293-299.
- Menter, F.R., *Best practice: scale-resolving simulations in ANSYS CFD*. ANSYS Germany GmbH, 2012: p. 1-70.
- Frere, A., et al. *Cross-validation of numerical and experimental studies of transitional airfoil performance*. in *33rd Wind Energy Symposium*. 2015.
- Anderson, J.D. and J. Wendt, *Computational fluid dynamics*. Vol. 206. 1995: Springer.
- LeBlanc, P., *An Experimental Investigation of Transitional Instabilities in Laminar Separation Bubble Flows on Airfoils Operating at Low Reynolds Numbers*. 1992, PhD Dissertation, University of Southern California.
- Liebeck, R. *Laminar separation bubbles and airfoil design at low Reynolds numbers*. in *10th Applied Aerodynamics Conference*. 1992.
- Gerakopoulos, R. and S. Yarusevich, *Novel time-resolved pressure measurements on an airfoil at a low Reynolds number*. AIAA journal, 2012. **50**(5): p. 1189-1200.
- Gerakopoulos, R., *Investing Flow over an Airfoil at Low Reynolds Numbers Using Novel Time-Resolved Surface Pressure Measurements*. 2011, University of Waterloo.